Polar low tracks over the Nordic Seas: a 14-winter climatic analysis

By MAXENCE ROJO[1,2], CHANTAL CLAUD[2]*, PAUL-ETIENNE MALLET[2],
GUNNAR NOER[3], ANDREW M. CARLETON[4,5] and MARIE VICOMTE[2],
[1]*Cultures, Environments, Arctique, Représentations, Climat, Observatoire de Versailles Saint-Quentin, Guyancourt, France*; [2]*Laboratoire de Météorologie Dynamique/IPSL, CNRS, Ecole Polytechnique, Palaiseau, France*; [3]*The Norwegian Meteorological Institute, Oslo, Norway*; [4]*Department of Geography, Penn State University, University Park, PA, USA*; [5]*Earth and Environmental Systems Institute, Penn State University, University Park, PA, USA*

ABSTRACT

To develop a 14-winter (October–April; 1999–2013) climatic description of polar low (PL) occurrence for the Nordic Seas, systems have been tracked using images acquired from the Very High Resolution Radiometer (AVHRR). Also, the dominant PL characteristics – their temporal and spatial distributions, size, lifespan, distance travelled, speed of propagation and directions – have been determined. On average, 14 PL events occur per winter but there is strong inter-annual and intra-seasonal variability. Although systems may form and travel over the whole Nordic Seas, their genesis is enhanced in areas characterised by warm oceanic currents. At the start of the season (October–November), systems mainly form over the Greenland and Norwegian Seas, but further into winter they form increasingly over the Barents Sea. In connection with recent low-ice winters, new areas of PL formation are evident, particularly to the west of Spitsbergen and in the Barents Sea. PL speeds of propagation range between 5 and 13 m/s but are observed to be highly variable among cases and even during the lifespan of individual PLs. To a considerable extent, the direction of movement is controlled by the large-scale flow in the lowest atmospheric layers, but we also observed cyclonic co-rotation of some pairs of PLs due to their influence on the ambient flow. Although these generally move southward or southeastward, a substantial number of PLs have westward and even northward tracks. PLs in the western part of the region average larger than their eastern counterparts. This study also highlights that PLs characteristics and tracks differ according to weather regimes.

Keywords: polar low, the Norwegian Sea, the Barents Sea, tracks, weather regime, sea-ice, dual and multiple systems

1. Introduction

During the winter season, polar mesoscale cyclones in cold air streams occur frequently over the Nordic Seas. The proximity of relatively warm open water to the cold snow-covered land masses and sea-ice, offer favourable conditions for the formation of these polar lows (PLs), which are the most intense of such mesoscale systems (Rasmussen and Turner, 2003). There are several definitions of PLs, however the following one is adopted in this study: 'A PL is a small but fairly intense low in cold air outbreaks (CAO) well north of the polar front, with a cyclonic cloud structure and a diameter of 200–600 km' (Heinemann and Claud, 1997; Noer and Lien, 2010).

PLs over Nordic Seas generally develop in zones of low-altitude baroclinic instability (e.g. near the ice margin of the eastern coast of Greenland and along the Barents ice edge), especially where there are large differences between air and sea-surface temperatures during CAO (e.g. Claud et al., 1992) traverse warmer ocean currents. Certain synoptic situations favour PL development, particularly those promoting instability due to condensational heating and sea surface–air heat fluxes, and within cold upper-lows that trigger positive vorticity advection (e.g. Businger, 1985; Claud et al., 2007; Blechschmidt et al., 2009; Mallet et al., 2013 for the Nordic Seas).

*Corresponding author.
email: chclaud@lmd.polytechnique.fr

1

This extreme weather phenomenon produces hazardous conditions that may impact coastal and maritime activities. Heavy snow and hail showers, strong wind gusts and squalls, high waves, icing, and thunderstorms are often associated with PLs (e.g. Dysthe and Harbitz, 1987). These hazards present potential risks to the growing maritime traffic, and also for the fishing and petroleum industries in the Norwegian and Barents Seas. In addition, the forecasting of PLs is particularly challenging due to their relatively small spatial and temporal scales: they can develop in a few hours, and be missed by the sparse network of synoptic observations covering the Arctic and sub-arctic seas.

A number of observation-based PL climatic studies for the Nordic Seas have been published, for example, Businger (1985), Wilhelmsen (1985), Ese et al. (1988), Harold et al. (1999), Bracegirdle and Gray (2008), Blechschmidt (2008), and Noer et al. (2011). Although informative as to PL typical patterns of development, movement and dissipation, these studies rely on several different definitions of the phenomenon, the study periods are generally short, and the study regions may be restricted. PLs have also been simulated and tracked in regional models through an automatic detection algorithm (Zahn and von Storch, 2008), although Laffineur et al. (2014) showed that not all PLs are represented in reanalyses even when a downscaling approach is used, and with some PLs missed or mis-identified. In this regard, Zappa et al. (2014) showed that an objective identification criterion disclosed 55% of observed PLs, but about 60% of those were not classified as PLs by those authors. For the present study, therefore, we use the relatively long-term climatic description of Noer and Lien (2010) recently updated to cover the 14-yr winter period (1999–2013), and which uses a consistent definition of PL, is based on the direct interpretation of satellite thermal infrared (TIR) imagery, and includes synoptic 'observations', scatterometer winds, surface radar data and output from a regional model (HIRLAM) with high spatial resolution ($0.2° \times 0.2°$) (see Subsection 2.1).

Although some basic characteristics of PLs – their distribution, size, type, lifespan, and so on – have been documented over the last three decades, their tracks of movement (e.g. Wilhelmsen, 1985; Eidsvik, 1987; Renfrew et al., 1997; Blechschmidt, 2008), which can provide critical information for risk management and hazard reduction issues, have received less attention. Track information can help identify typical patterns of movement of PLs, as well as their intra-seasonal and inter-annual variability; all potentially important for clarifying PLs' role as a maritime hazard. The scarce information about PL tracks and their dominant directions and speeds of propagation over a reasonably large number of winters, are key motivators of this study.

Accordingly, this paper presents a 14-winter climatic analysis of PL tracks for the Nordic Seas, with a statistical description of PL dominant characteristics that includes their associations with 'weather regimes' (WRs) (Mallet et al., 2013) and also considers their inter-annual variability. Attributes of dual and multiple PLs are analysed and presented. For these purposes, we tracked PLs by observing the associated cloud signatures on satellite TIR imagery; this approach permits a relatively precise manual tracking for higher-latitude regions (as in Fitch and Carleton, 1991; Carleton, 1995).

Specific improvements in our study compared to previous PL studies for the Nordic Seas are as follows:

- The database is longer and contains a much larger number of PL events than previous manual observational analyses (e.g. Wilhelmsen, 1985; Blechschmidt, 2008), including that of Noer et al. (2011). The longer record permits us to better study PL inter-annual variations;
- We emphasise the tracks of larger numbers of PLs from genesis to decay, their sub-regional variations, and associations with low frequency atmospheric circulation patterns (WRs) and the lower tropospheric flow;
- The evolution of PL characteristics from genesis to decay – particularly the size and lifespan attributes – is documented;
- In case of dual and multiple PL, we investigate the characteristics of auxiliary systems.

The structure of the paper is as follows. Section 2 describes the data and methods of analysis. In Section 3 the dominant attributes of PLs are described, followed by PL lifespan characteristics. Then, Section 4 discusses the results and their significance. A summary of the results is given in the final section.

2. Data and methods of analysis

We conducted manual tracking of PLs, and determined PL dominant characteristics, for the 14-yr (1999–2013) winter period using the following data sources: (1) a listing of mature PLs from the Norwegian Meteorological Institute (MET-Norway); (2) the identification and characterisation of cloud signatures associated with PLs using mainly those acquired from the Very High Resolution Radiometer (AVHRR) TIR imagery; and (3) atmospheric reanalysis data to clarify PL associations with the larger-scale circulation. Fuller details are provided in Subsections 2.1 and 2.4.

2.1. Updated list of PL occurrences

The 14-winter climatic description of PL tracks and statistics of other PL attributes for the Nordic Seas, are based on the annual listing of all PL activity published by the

Norwegian Meteorological Institute (MET-Norway) in Tromso since 1999 (Noer and Lien, 2010). This list covers an area extending from the Greenland east coast to Novaya Zemlya in longitude, and from 65°N to the Arctic ice edge in latitude. The list gives the date and position of every PL at its mature stage, when the cloud structure displays a pronounced vortex with cloud free eye, for the period September 1999 to May 2013. It also provides the minimum MSLP and the maximum near-surface wind speed for those PLs when these data are available.

Because the studied area is sparsely covered by synoptic observations, the main source of information for the PL list comes from the interpretation of TIR AVHRR imagery that is available multiple times per day for these latitudes. Data on scatterometer winds (ASCAT), Sea Winds Scatterometer (QuikSCAT), and surface radar and buoy data, also yield information for PLs over the Norwegian and Barents Seas.

Because the definition of PLs could easily include small-scale extra-tropical cyclones, the formation process of the system is considered to avoid false identification. The PL is uniquely associated with a CAO from the polar ice. In contrast, small waves on the polar front with developing warm and cold fronts that have baroclinic instability as their main source of energy, may have a similar size to the PL, but because the air masses in which they develop have different characteristics from the more statically unstable air mass typical of PLs, they are not so classified. Other similar phenomena, for example, the surface troughs can be similar to a PL in terms of resulting weather, but are of generally lower intensity. They are easily identified from a linear appearance, as opposed to the vortical shape of the PL. These polar troughs do not need the enhancement from upper layers to develop, are therefore far more common than PLs, and so are classified differently. Deterministic Numerical Weather Prediction (NWP) models such as the Hirlam 8 or 12 km model, or the European Centre for Medium-Range Weather Forecasts (ECMWF) operational model are used by Noer and Lien (2010) to differentiate PLs from other similar-looking phenomena. Indeed, NWP models provide information on key parameters such as sea surface temperature (SST), the nature and history of the air mass at low levels, the vertical temperature distribution, the cold cores in the middle troposphere, inversion levels and the nature and baroclinicity of any given frontal zones in the PL area; this information provides a sufficient understanding of the state of the atmosphere to be able to correctly classify PLs.

NWP models are also used by MET-Norway for the MSLP analysis, which are then corrected to fit synoptic observations. This is especially useful for the analysis over scarcely covered areas like the sea areas in the Nordic Seas. The MSLP data for the Noer and Lien (2010) list are taken from the daily analysis at the MET-Norway. Unless the low has passed directly over a synoptic observation point, the pressure is approximated, because of the sparse conventional observations, but should be within about 3 hPa. The lowest MSLP of a PL typically occurs some 3–9 hours after first identification of the PL on satellite imagery (Noer and Lien, 2010).

Satellite images reveal several possible cloud signature types associated with PLs (e.g. in Carleton, 1985, 1987, 1995, 1996). In the present research, most PLs are either spiraliform or comma shaped, but they are not distinguished here for purposes of this PL track study.

For PLs occurring in pairs or as clusters of multiple low-pressure centres, only data on the deepest low of the system are recorded in the list, but a comment is included to indicate that this is one of multiple circulations (Noer and Lien, 2010).

Based on this PL list, which provides only one location for each PL, we tracked all events (190 events) occurring in the 14 winter seasons 1999–2000 to 2012–2013. We note that 40% (80 events) of those PLs are dual or multiple (with at least three PLs) systems. Very often, several vortices form approximately at the same image time and in the same general vicinity of the main vortex, but it is not certain that all vortices reach a sufficient wind speed to be considered as PLs. In this study, occurrences of between two to more than five vortices at around the same time emphasise the wide variety of dual and multiple systems. The range of cloud signatures comprising multiple PL systems is illustrated in Fig. 1. Figure 1e. and f. highlights the complexity of some multiple PL events. From those multiple PL events, merry-go-round systems can be the most difficult to track and analyse individually. For PL outbreaks of multiple vortices (Section 3), only the main vortex is considered when deriving statistics on PL temporal and spatial distributions, size, lifespan, distance travelled, and speed of propagation and direction, because of the lack of information on the wind speed reached by each vortex. We acknowledge that the exclusion or inclusion of auxiliary PL systems may lead to biases in the statistical analysis of PL occurrence and characteristics. However, the statistical analysis of dual and multiple systems, discussed in Section 4, reveals their broadly similar spatio-temporal characteristics to the main vortices.

2.2. PL observations from AVHRR imagery

Based on the MET-Norway list, we manually determined the tracks of all PLs using the freely accessible archive of AVHRR – TIR Channel 4 (10.3–11.3 µm) images provided by the UK's Natural Environment Research Council (NERC). The University of Dundee's NERC Satellite Receiving Station corrects the effects of earth curvature, and superimposes a 10° latitude–longitude grid and coastlines onto the images. The spatial resolution is approximately 1 km at nadir for the TIR (http://www.sat.dundee.ac.uk/freeimages.html).
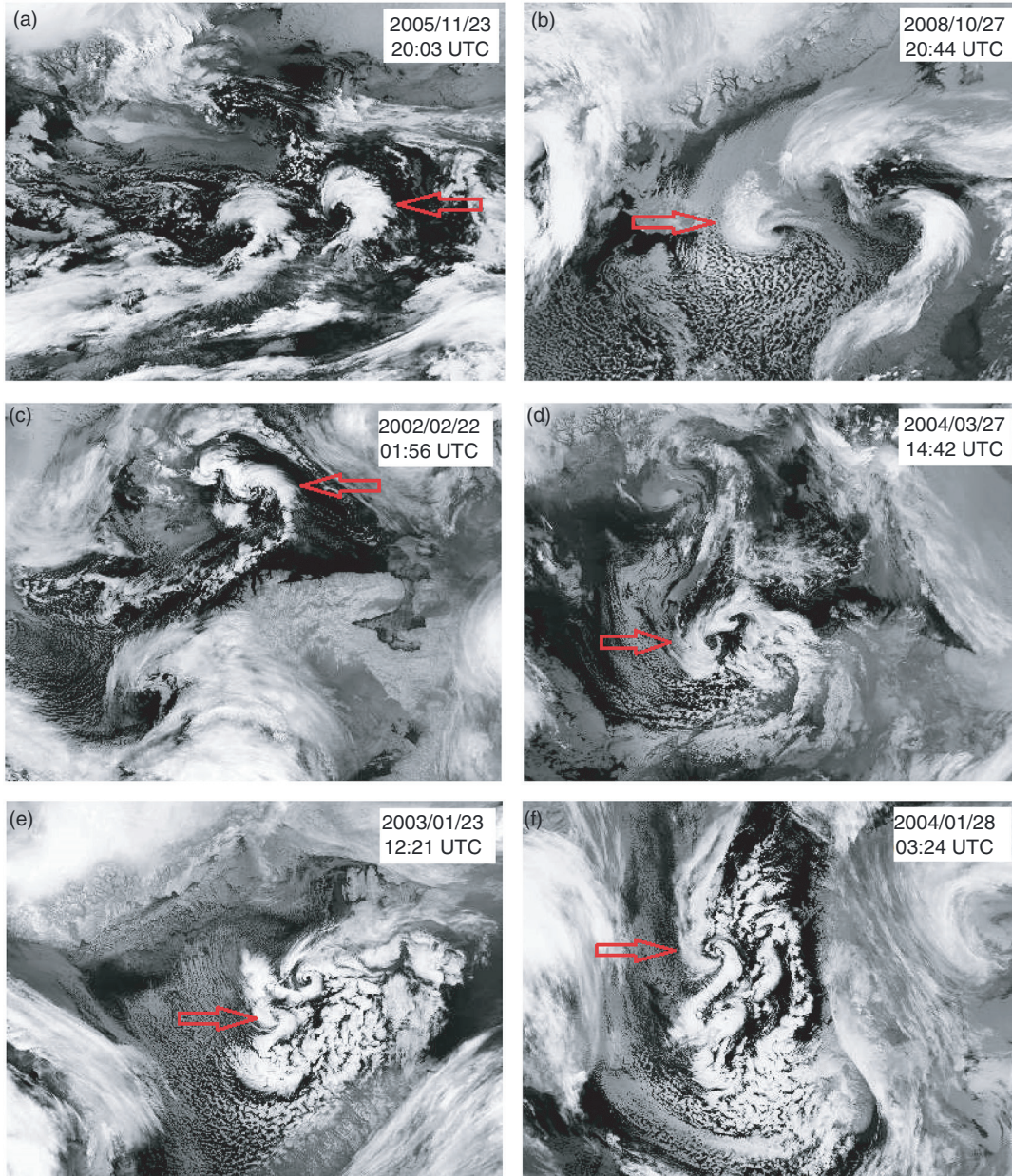
Fig. 1. Different examples of multiple systems: (a) a dual system, (b) a multiple system, (c) and (d) wave systems and (e) and (f) merry-go-round systems. Red arrows show the deepest lows.

These images also permit estimation of the location, duration and diameter of PLs, from tracking of the associated cloud vortex signatures. When necessary (i.e. for tracking the easternmost occurring PL events), satellite images of the Barents Sea were acquired from the Space Research Institute of Russian Academy of Sciences (http://smisdata.iki.rssi.ru/data/noaa/html/cat_tlm.shtml).

On average, satellite images are available every 3 hours (±1.5). In about 60% of PL cases there is a gap of 2 hours

or less between each AVHRR observation of a PL, and in less than 5% of cases does a gap exceed 7 hours.

2.3. Atmospheric Reanalyses and WRs

Determining the lower troposphere wind field (i.e. speed and direction) associated with each manually-derived PL track relies upon the ECMWF Re-Analysis Interim (ERA-I) wind fields at 850 and 925 hPa. ERA-I is the latest ECMWF

global atmospheric reanalysis, covering the period 1979 to present on 37 vertical levels with a $0.75°$ latitude $× 0.75°$ longitude grid resolution and a 6-hourly temporal resolution (Dee et al., 2011).

We determine the Arctic sea-ice extent using the Operational Sea Surface Temperature and Sea Ice Analysis system (OSTIA) from the National Centre for Ocean Forecasting (NCOF). This product yields SST at $0.05°$ latitude $× 0.05°$ longitude horizontal resolution, using in-situ data and satellite retrievals from both TIR and microwave radiometers.

Mallet et al. (2013) documented the associations of observed PLs in the Noer and Lien (2010) shorter list (1999–2009) with North Atlantic–Europe WRs over the Nordic Seas. The four most common large-scale flow patterns pertinent to the cold season (November–March) are as follows: Scandinavian Blocking (SB); the positive and negative phases of the North Atlantic Oscillation (NAO); and a pronounced ridge over the Atlantic (Atlantic Ridge; AR) (e.g. Cassou, 2008). We used the daily mean values of 500 hPa heights (Z500) from the NCEP/NCAR Reanalysis to determine the WR associated with each PL of the updated list using the NCEP/NCAR Reanalysis, which covers the period 1948 to present on 17 pressure levels at an approximate $2°$ grid resolution (Kalnay et al., 1996). We determined the daily WR accompanying each PL for all PL wintertime events (November–March) of 1999–2013 over the North Atlantic–Europe domain ($20°$N–$80°$N/$90°$W–$30°$E). For the discussion based on WR type, PLs that form in September–October and in April–May are therefore classified as 'Others' (30 cases out of 190 PLs observed) because they occur outside the time of year when the WRs are well defined.

2.4. Determination of PL tracks and other attributes

We tracked the full lifespan of PLs, from genesis to dissipation, on the TIR AVHRR imagery. The updated Noer and Lien (2010) list provides only one date and location per PL. From this single position we found all crossing points for each PL listed. To determine genesis and dissipation points and also the trajectories of all PLs, we analysed all TIR AVHRR images available between 48 hours before and after the dates and positions of mature PLs provided by the updated list. PL genesis corresponds to the first image on which a clearly formed cyclonic cloud vortex is present. We consider PL dissipation to occur when a cyclonic cloud circulation is no longer evident. To be considered for tracking, the PL centre should be clearly evident on all satellite images.

In nine PL cases (out of 190 total), the formation or dissipation phases could not be observed because the temporal spacing of images did not allow tracking of such rapidly evolving systems for their entire lifespan. Despite the fact that these tracks are probably abbreviated, we still consider them in this study.

The PL tracks we derive give the best estimated position of PL centres from genesis to decay. The PL position corresponds to the centre of a cloud vortex that may include an eye. When an eye is not clearly evident or when the cloud band is only weakly curved, the approximate periphery of circulation is determined subjectively, to denote the PL centre.

The size of a PL can be difficult to estimate; it may change during the lifespan of the low, particularly as the associated cloud patterns take on different forms (spiraliform, comma shaped, etc., see below). Here, the size of the PL is defined by the diameter of a circle that forms the PL cloud vortex during its mature phase, at the time when the PL is first identified as a fully developed circulation. When the eye is clearly visible, it is possible that the centre of the PL differs a little in location from the geometrical centre of its periphery. Only the cloud vortex is included for calculating PL diameter; the cloud-band tails of comma-shaped systems are excluded from consideration in our analysis. An example of the tracking procedure is presented for the PL of 24 March 2000 in Fig. 2, from the successive positions deduced from the available satellite images. We observe on early images (Fig. 2a, b and c), a comma-shaped PL forming between the Svalbard archipelago and Norway. Figure 2d highlights the transition from comma shaped to spiraliform PL. As the PL moves southeastward, its diameter increases slightly until the dissipation stage. On the last AVHRR image (Fig. 2g), the PL decays over the coast of Finnmark (northern Norway). This interpretation procedure results in the track shown in Fig. 2h, and also illustrates how a PL may vary in terms of vortex size and form during its lifespan.

Our manual tracking of PLs also allows determination of their dynamical characteristics, such as: duration, distance travelled, speed of propagation and direction. In our study, the approximate duration corresponds to the time between the first and last satellite observations of the PL vortex. For presentation purposes, we classify duration into nine categories, from less than 6 hours to more than 48 hours, by 6-hour intervals. The distance travelled includes the total distance between each pair of points forming a track segment (i.e. total distance travelled) between the first and last observations of each PL. Adding the distance between all points along the PL track gives the total distance travelled, which limits the biases associated with curved tracks.

The PL speed of propagation is estimated by dividing the total distance travelled by the system approximate duration. Finally, the main direction refers to the straight line connecting the starting and ending points. We classify directions into 16 categories each of $22.5°$ interval.
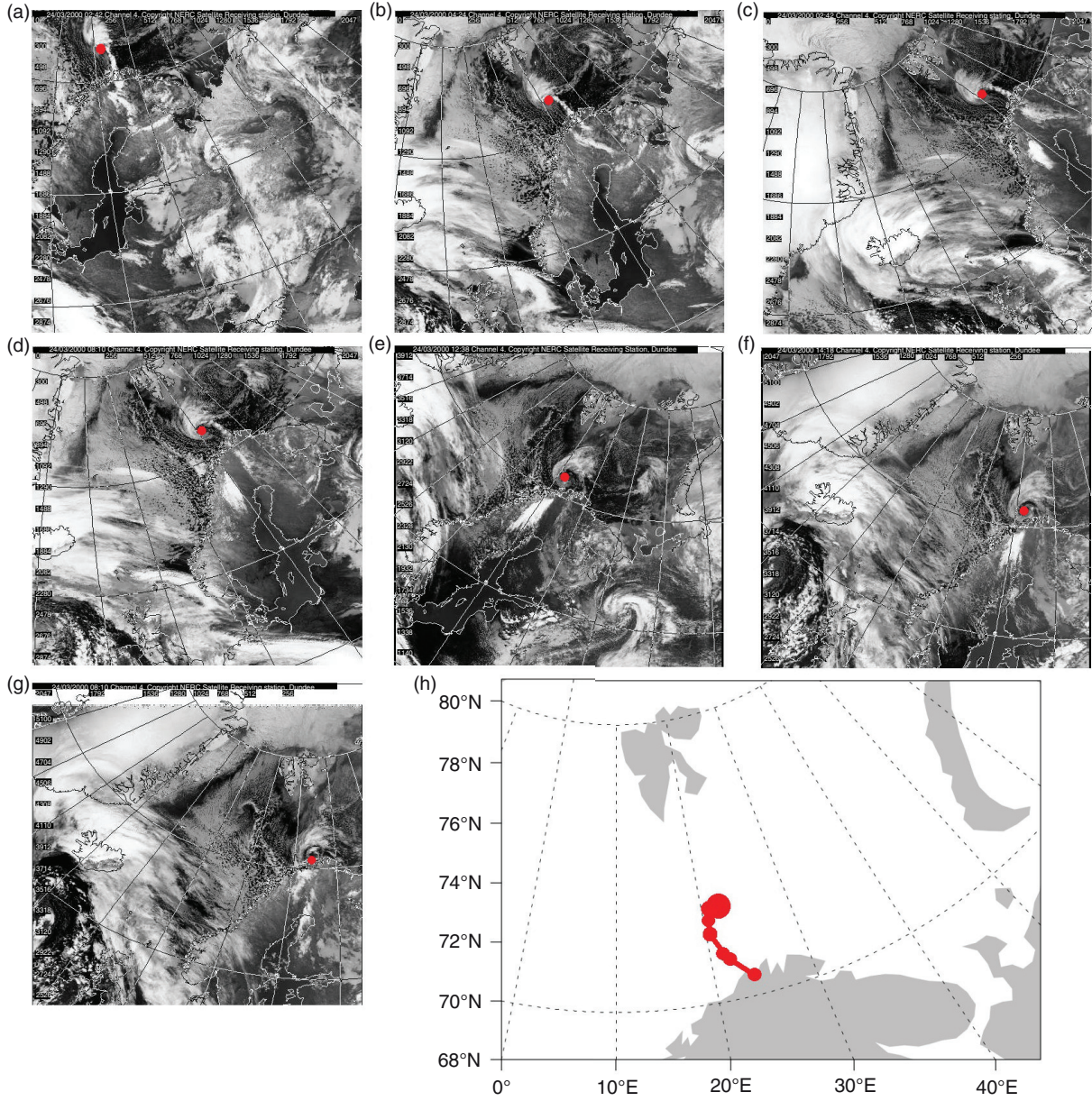
Fig. 2. Example of a PL manual tracking using AVHRR images for the PL event of 24/03/2000. On initial images (a, b and c), a comma-shaped PL forms between Svalbard and Norway. As it moves southward, the PL changes to a spiraliform system (transition stage on image (d)). On the last image (g), the PL decays over the coast of Finnmark (Norway). Red points show the centre of the PL. Image h shows the approximate track of this PL event.

3. Results

3.1. Basic attributes of PLs over the Nordic Seas

3.1.1. Temporal distribution. PL formation over the Nordic Seas is characterised by strong inter-annual varia-bility (Fig. 3). On average, there are approximately 14 PLs per winter for the full period, ranging from a maximum of 23 in 2012–2013 to a minimum of 5 in 1999–2000. The

standard deviation is approximately 6. This result differs notably from the study by Blechschmidt (2008) who ob-served about 90 PLs over a 2-yr period.

The monthly distribution of PLs for each winter between 1999–2000 and 2012–2013 is shown in Table 1. Because months contain different numbers of days, the monthly distribution has been normalised by multiplying the average daily frequency per month by 30. Table 1 confirms that the PL season runs from October to April, with an overall
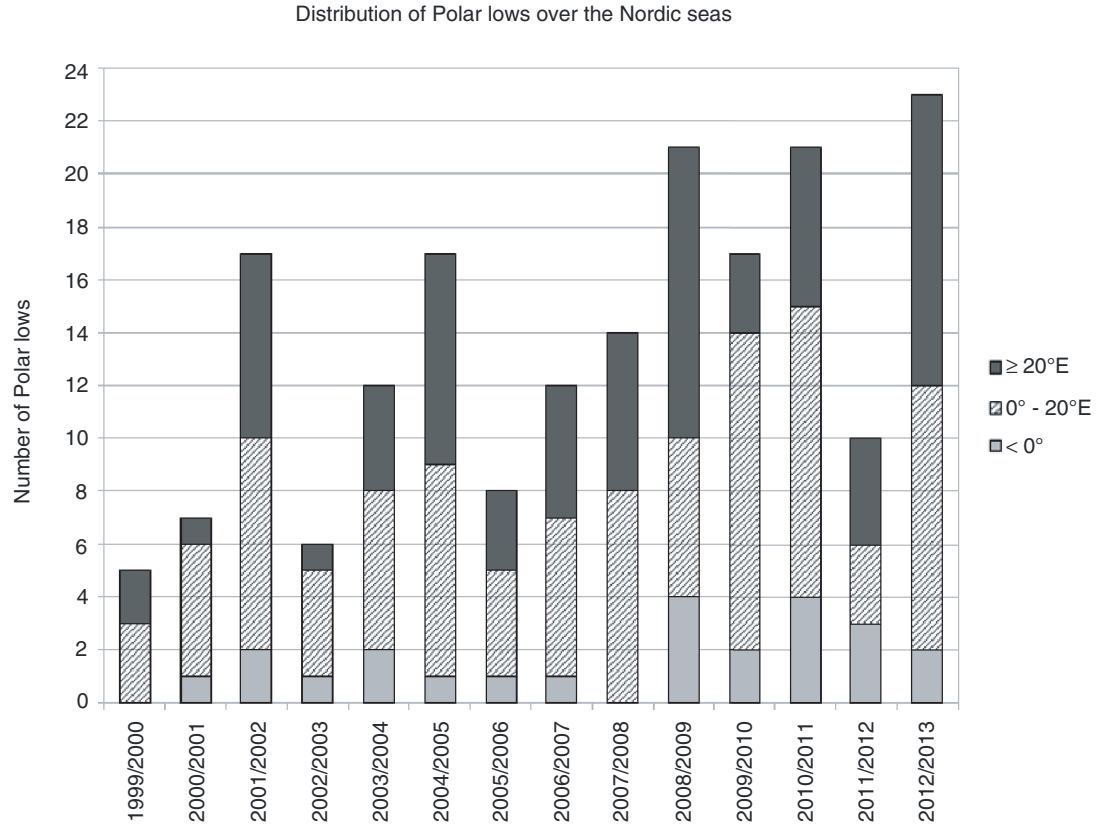
Distribution of Polar lows over the Nordic seas

Fig. 3. Inter-annual variability of PLs over the Nordic Seas from winter 1999/2000 to winter 2012/2013. Polar lows that form over the Greenland Sea (west of 0°) are represented in light grey, those that form over the Norwegian Sea (between 0° and 20°E) are represented in striped black and white and those that form over the Barents Sea (east of 20°E) are represented in dark grey.

maximum in March. We note that a fully developed PL was observed in early September along the Norwegian coast (3 September 2007), and two PLs were observed over the

Norwegian Sea in May (20 May 2002 and 31 May 2010), during the study period. Nevertheless, it should be empha- sised that the monthly frequency distribution of PLs is

Table 1. Monthly distribution of observed PLs over Nordic Seas for the 14-winter period

	September	October	November	December	January	February	March	April	May	Total
1999/2000	–	–	–	1	2	–	2	–	–	5
2000/2001	–	–	–	–	1	2	3	1	–	7
2001/2002	–	1	4	1	5	3	2	–	1	17
2002/2003	–	–	–	1	3	–	2	–	–	6
2003/2004	–	1	–	5	2	2	2	–	–	12
2004/2005	–	–	5	2	3	1	4	2	–	17
2005/2006	–	1	2	1	1	–	3	–	–	8
2006/2007	–	1	1	2	4	2	–	2	–	12
2007/2008	1	–	–	1	2	2	6	2	–	14
2008/2009	–	1	6	1	3	5	1	4	–	21
2009/2010	–	–	–	–	3	3	9	1	1	17
2010/2011	–	2	3	3	3	2	8	–	–	21
2011/2012	–	–	1	2	–	2	3	2	–	10
2012/2013	–	1	–	1	1	2	13	5	–	23
Total	1	8	22	21	33	26	58	19	2	190
Average frequency	0.07	0.57	1.62	1.50	2.36	2.04	4.14	1.40	0.14	13.57

highly variable. In particular, the most prolific month for PLs (March) is also the most variable, with no PLs in 2007 yet 13 PLs in 2013 (Table 1); indeed, the number in the latter winter is even higher given several multiple PL events.

To better analyse the sub-seasonal evolution of PLs we distinguish two 7-yr sub-periods. The first sub-period extends from September 1999 to May 2006, gives broadly similar results to Noer et al. (2011) study, with maxima in January and March, a local maximum in November, and a minimum in February (Fig. 4a). For the second period (September 2006 to May 2013), the frequency of PLs is high from January to April, without a local minimum in February and there are as many PLs in April as in January (Fig. 4b).

Thus, the seasonal distributions of PLs are different between the two sub-periods without any change in data availability or in the analysis technique (Fig. 4).

3.1.2. Tracks of PLs. PL tracks from December 1999 to April 2013, determined using the method described in Section 2.4 and stratified by month, are displayed in Fig. 5. PLs develop and travel over all open-water areas of the Nordic Seas. Most PLs decay when they reach the coasts of Norway or the Kola Peninsula. Nevertheless, there are instances of PLs that retained their cyclonic structure even after landfall, although they no longer had associated strong
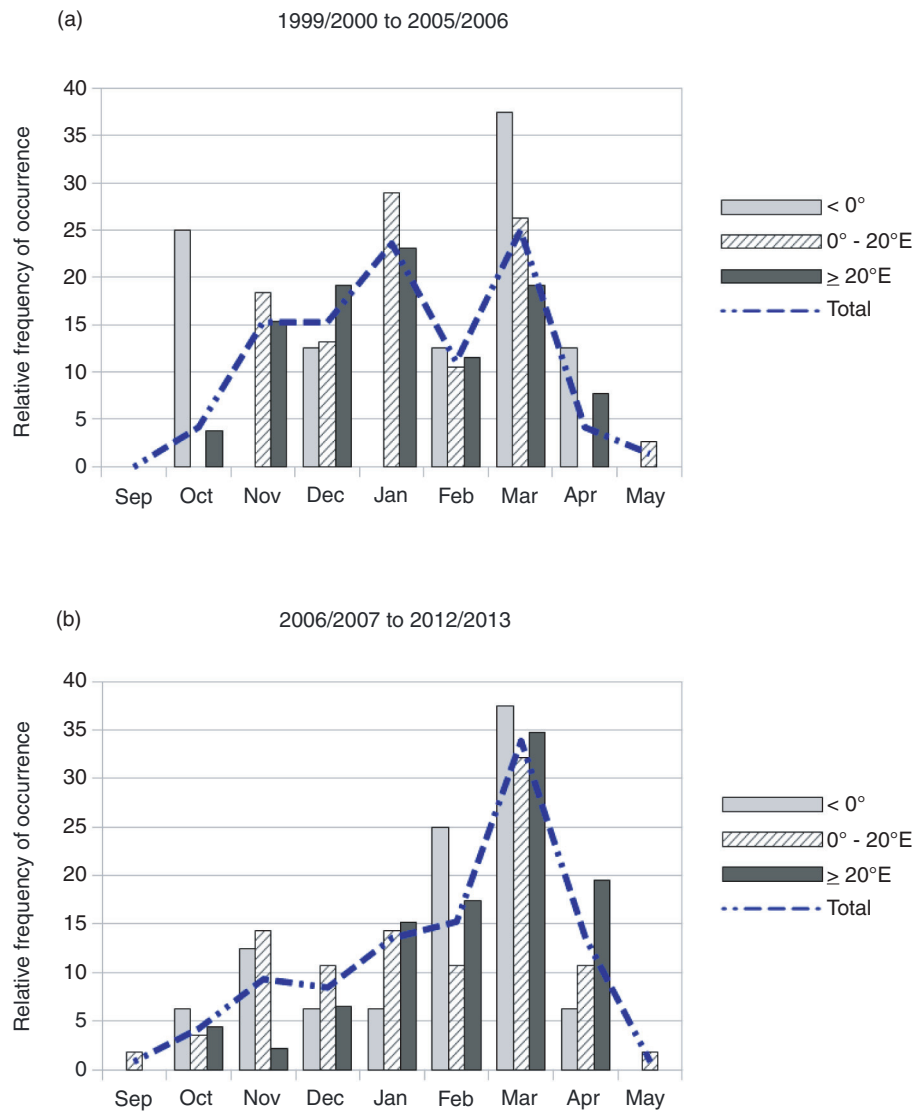

Fig. 4. Monthly distribution of PLs over Nordic Seas found from (a) winter 1999/2000 to winter 2005/2006 and (b) winter 2006/2007 to winter 2012/2013. Number of PLs per category for the period 1999/2006: eight PLs for $\leq 0°$, 38 PLs for $>0°-20°E$ <and 26 PLs for $\geq 20°E$. Number of PLs per category for the period 2006/2013: 16 PLs for $\leq 0°$, 56 PLs for $>0°-20°E$ <and 46 PLs for $\geq 20°E$.
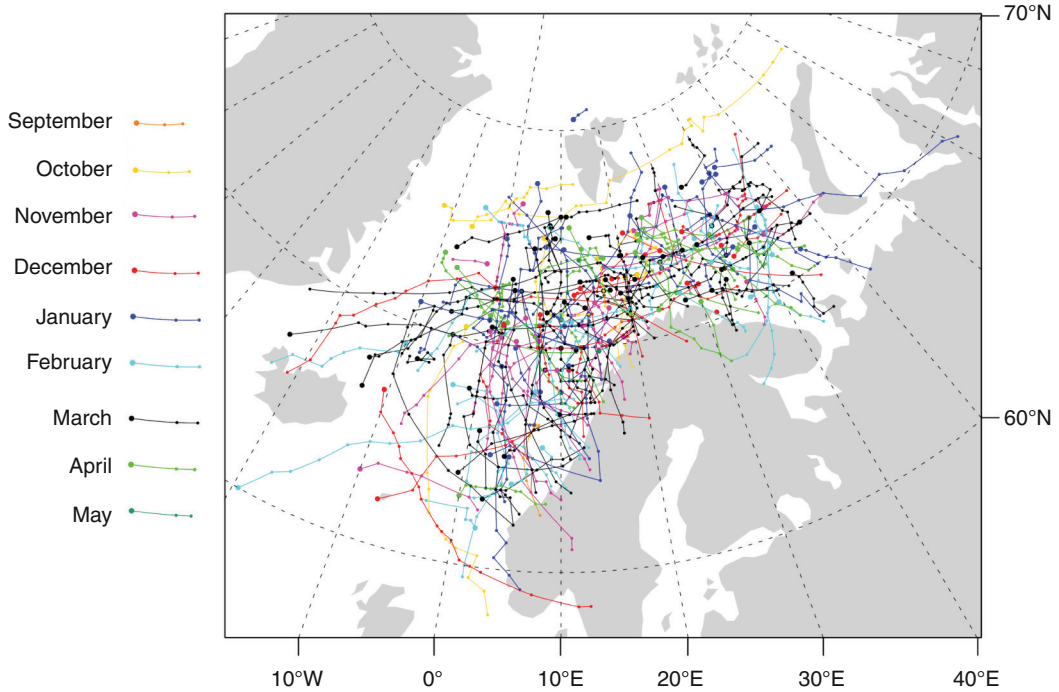
Fig. 5. The diagnosed 14-yr (winters 1999/2000 to 2012/13) polar low tracks over the Nordic Seas.

surface winds. Our 14-winter manual tracking of PLs shows that the spatial distribution changes during the season of PL. Indeed, our study suggests that in autumn, at the start of the season, most systems form over the Greenland and Norwegian Seas. During the winter peak period, the tracks give the impression that PL development expands to include the Norwegian and Barents Seas. In spring (April) when the season is ending, most PLs seem to form over the Barents Sea. PL activity over the Greenland Sea is greatest in October, February and March. Over the Norwegian Sea, PLs attain higher frequencies in November, January and March. The number of PLs that form over the Barents Sea increases between January and April (Fig. 4).

In recent years, the reduced sea-ice extent in winter and its later formation in autumn apparently have allowed a spatial extension of the area of PL genesis; in particular, in the north of the Barents Sea and over the Greenland Sea compared to the 1980s and 1990s (Comiso, 2011; Årthun et al., 2012). One case serves to illustrate this wider expansion of PL development in the winter. On 8 January 2010 the northernmost PL ever observed formed north of Svalbard archipelago at a latitude exceeding 80.5°N (Fig. 6). This system could have resulted from the unusual absence of sea-ice around Svalbard, whereby exposed ocean would have increased heat fluxes into the atmosphere and enhanced static instability. On 16 January 2009, a PL moved over the Kara Sea and travelled towards the Yamal Peninsula (until 63.5°E longitude). Again, this unusually poleward case could have resulted, at least in part, from an absence of sea-ice over the

Kara Sea between Novaya Zemlya and the Yamal Peninsula (not shown).

To determine sub-regional scale variations of PL genesis locations, we divided the study area into 86 grid cells each of 2.5° latitude by 5° longitude. The normalised density of PLs forming in each grid cell, with the oceanic surface currents superimposed, is given in Fig. 7. The number of PLs per winter is normalised to an equal unit area (50 000 km^2). Note that a higher PL density coincides with the warm ocean currents (WAC) of the Norwegian and Barents Seas. PL density is greatest at the convergence of the Norwegian Atlantic Current (NAC) and the West Spitsbergen Current (WSC), and the NAC and Barents Sea currents. About 25% of PLs form in areas relatively close to the ice edge.

The recent lengthening of the PL season (Section 3.1.1) is also accompanied by spatial changes in PL occurrence. The PL increase occurs widely for the Nordic Seas, but appears to be greater over the Greenland Sea, especially along the West Spitsbergen coast (74°N–81°N latitude, and 0°–17°E in longitude), and also over the Barents Sea (between 70°N–74°N and 20°E–40°E).

Figure 8 displays the diagnosed 14-winter PL tracks over the Nordic Seas according to WRs. Mallet et al. (2013) showed a relationship between WRs and PL occurrence, but Fig. 8 indicates that the tracks of PLs also differ according to WRs. We note a wider area of PL formation and development, especially for the negative and positive phases of the NAO during the period 2006/2013. During the AR configuration, PLs form in narrower areas, such as closer to the
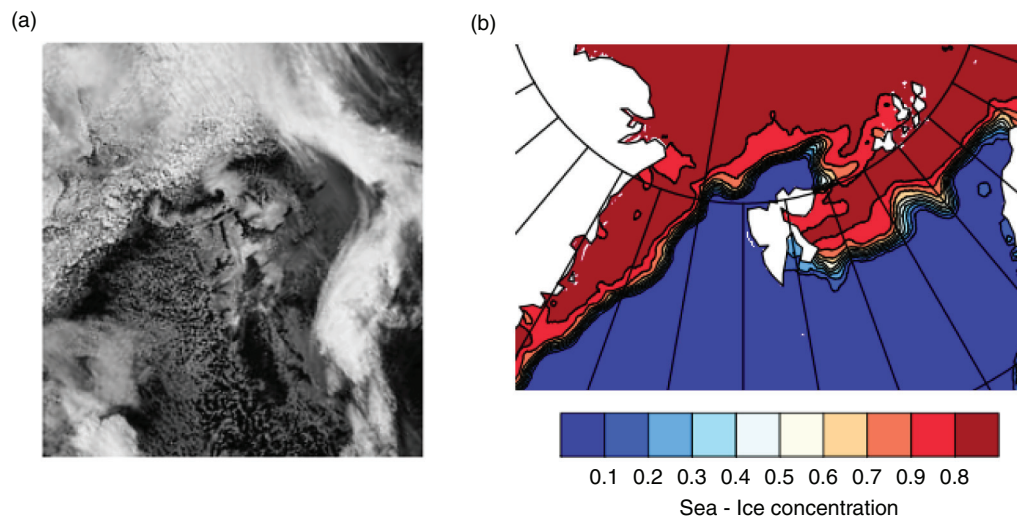
(a)   (b)

0.1 0.2 0.3 0.4 0.5 0.6 0.7 0.9 0.8
Sea - Ice concentration

Fig. 6. (a) Image TIR AVHRR showing the northernmost case of PL, 8 January 2010 at 11:08 UTC. (b) Sea-ice concentration for the day 8 January 2010, data from OSTIA.
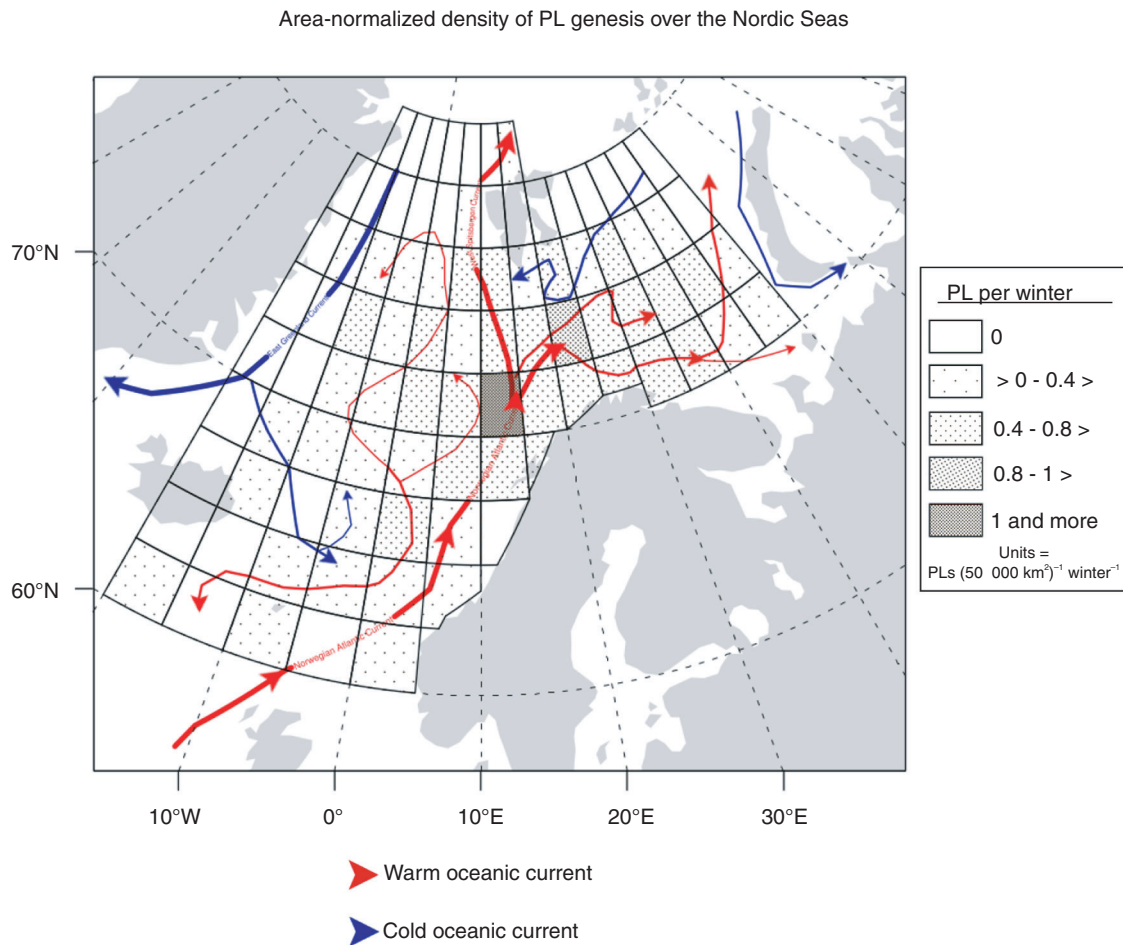
Area-normalized density of PL genesis over the Nordic Seas

Fig. 7. Area of PLs genesis over the Nordic Seas from winter 1999/2000 to winter 2012/2013. Normalised distribution per winter [Units = PLs $(50\,000\,\mathrm{km}^2)^{-1}$ winter^{-1}]. Red and blue arrows show approximately the warm and cold ocean currents for the region of investigation.
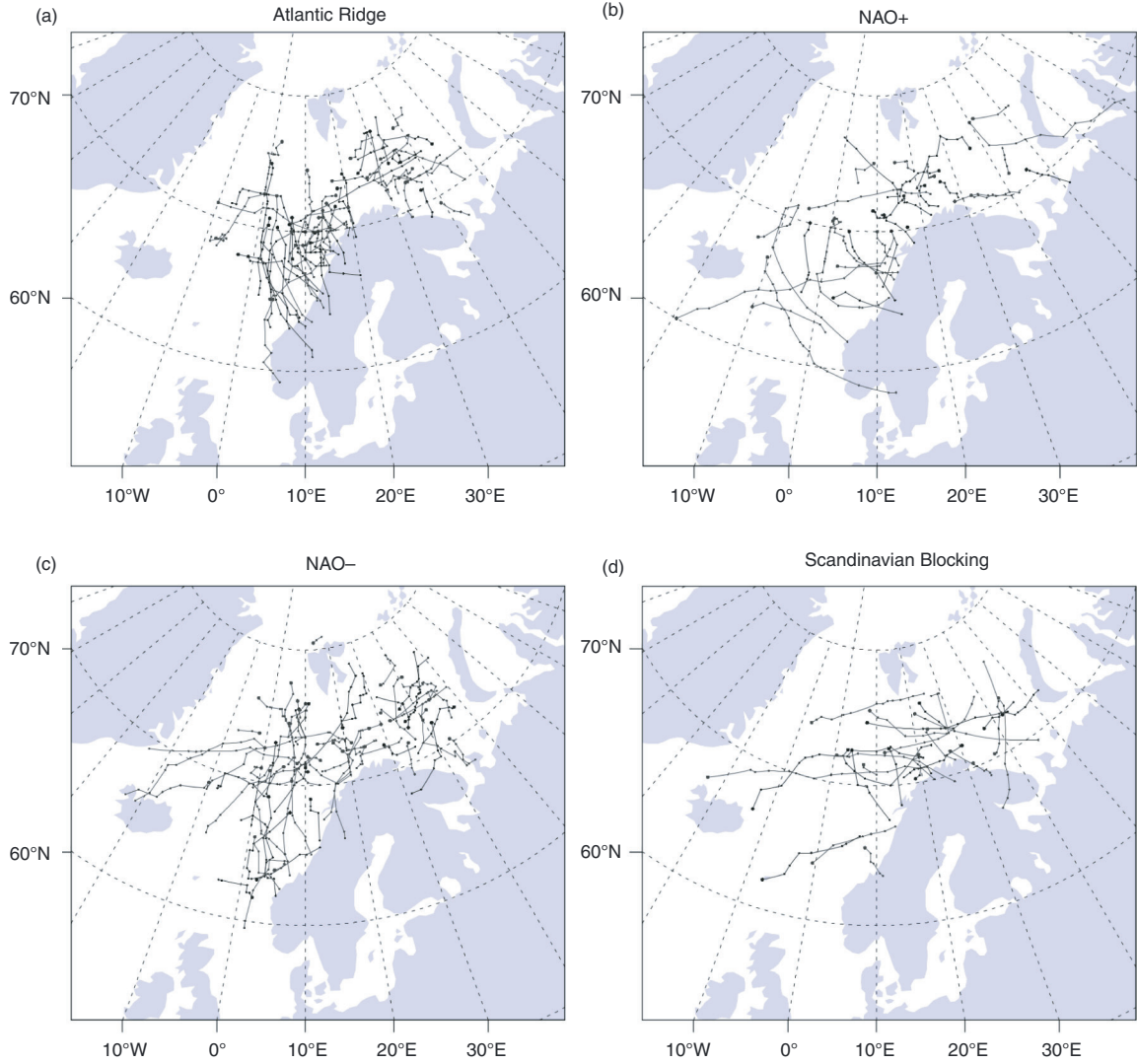
Fig. 8. The diagnosed 14-winter polar low tracks over the Nordic Seas according to weather regimes. (a) Atlantic Ridge, (b) NAO+, (c) NAO − and (d) Scandinavian Blocking.

Norwegian and Russian coasts, and possibly make landfall more often than during other WR configurations. A more detailed analysis of links between WRs and PL directions will be provided in Section 3.2.

3.1.3. PL size. For the study period, PLs exhibit a continuous spectrum of sizes at the mature stage, ranging from 150 to 600 km, even reaching 850 km on occasion (Fig. 9a). The PL mean diameter is 350 km, and 64% of fully developed PLs are distributed between 250 and 450 km. PL size can vary during system lifetime, and diameters can more than double between the formation and dissipation stages. We note also that the form of PL can change during system lifetime (33%).

Forty-two per cent of PLs increase in size during their lifetime. Twenty-six per cent of observed PLs grew until the mature stage and then decreased in size during the dissipation stage. However, 20% of PLs exhibit diameters that change inconsistently as they evolve. In most cases (72%) PLs are biggest during the dissipation stage, in agreement with Harold et al. (1999) for meso-cyclones over the North-East Atlantic. Only 12% of observed PLs in our study do not change appreciably in size during their lifetime.

Spatial differences in the size of PLs appear according to their area of genesis. PLs that form over the Greenland and Iceland seas (0°W to 20°W) are generally larger than those elsewhere. More than half of PLs that form between 0°W and 20°W exhibit diameters of 450 km or more, while 80% of PLs that form east of 0° longitude are smaller than 450 km (Fig. 9a). PLs forming over the Barents Sea (20°E to 50°E) average smaller, with 65% smaller than 350 km.
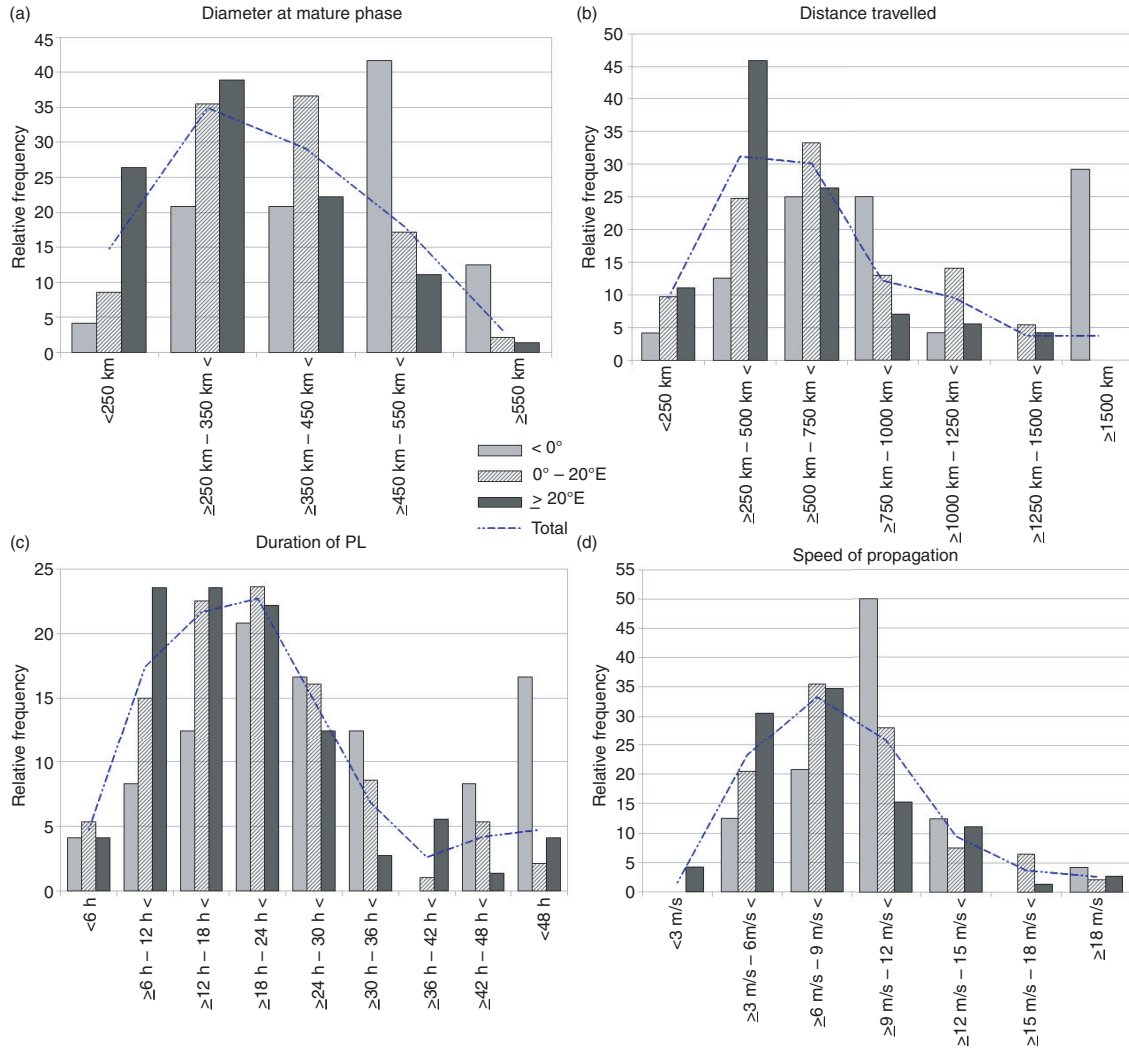
Fig. 9. PLs characteristics according to their genesis areas. (a) diameters, (b) total distance travelled, (c) lifespan and (d) speed of propagation. Number of PLs per category: $\leq 0°$ (24 PLs), $> 0°$–20°E $<$(94 PLs), $\geq 20°E$ (72 PLs) and Total (190 PLs).

PLs forming during the positive and negative phases of the NAO average smaller diameters than during other configurations (Fig. 10a). This characteristic is more marked during the NAO $-$, with more than 60% of PLs smaller than 350 km and only 11% reaching 450 km or more at the mature phase. Conversely, more than 30% of PLs that form during SB configuration are bigger than 450 km.

3.2. Lifespan attributes of PLs

3.2.1. Duration and distance travelled. PLs forming over Nordic Seas for the full study period lasted between a few hours to more than 72 hours. Two-thirds (67%) of PLs lasted less than 24 hours. Most PLs (77%) are distributed between 6 and 30 hours. Although rare, some PL events can exceed 48 hours (nine events, or less than 5%) (Fig. 9c).

The longest PL observed in this study occurred on 5 April 2012, and lasted more than 3 d. The cloud cover associated with this event could be observed for at least 76 hours. A PL forming over the Norwegian Sea in October 1993 also lasted for about 3 d, and was studied in detail (e.g. by Claud et al., 2004). We note that the mean time interval between the early and mature stages in our study is 7–8 hours.

Nordic Sea PLs can travel up to 2000 km, although most travelled fewer than 1000 km (83%), and 61% of observed PLs travelled between 250 and 750 km (Fig. 9b). The longest distance travelled by a PL in this study occurred on 27 October 2001; it formed along the ice margin of Greenland's east coast and dissipated north of the Kara Sea between Novaya Zemlya and Severnaya Zemlya archipelagos, for a total distance of 2400 km. There are differences in PL distance travelled according to area of genesis. On average,

PLs that form in the western part of the area (0°–20°W) have longer lifetimes and travel greater distances (Fig. 8c and 9b). The briefest and shortest-travelled PLs tend to be those that form close to the coast of Norway and the Kola Peninsula. Because PLs decay rapidly when making landfall, the proximity of the genesis area to the Norway and Kola Peninsula coasts is likely the major reason for the short system duration, small size and reduced track length.

PLs accompanying the AR WR have a narrower distribution in terms of distance travelled and duration than those for other WR configurations. Indeed, more than 95% of AR PL tracks are 250–1250 km long, and no tracks are longer than 1250 km. Moreover, 92% of AR range from 6 to 30 hours (Fig. 10b and c). The SB configuration seems to favour two different types of tracks. First are short-lived and travel short distance. Figure 10b and c show that more than 40% of these PLs travel less than 500 km and dissipate before 12 hours. The second type of SB PL tracks average longer distances than PL tracks accompanying other WRs, with 30% travelling 1000 km or more (respectively 12%, 19%, 19% and 13% for AR, NAO+, NAO− and Others). We note that this second type of SB PLs are bigger than for other WRs as mentioned earlier in Section 3.1.3, but they do not average longer lifespans, which can be explained by their relatively fast speeds of propagation (see Section 3.2.2).

We also investigate the possible links between PL size, duration and distance travelled. We classified PL size in the mature stage into three categories to facilitate statistical analysis: less than 300 km (72 PLs), 300 km to less than 400 km (60 PLs), and more than 400 km (57 PLs) (Fig. 11). The median duration for these size categories is 15.5 hours, 19 hours and 23.5 hours respectively, and the corresponding median distance travelled is 400 km, 600 km and 700 km. Fifty per cent of the biggest PLs travel 700 km or more, while less than 20% of the smallest PLs travel more than 700 km. More than 80% of the smallest PLs do not last beyond 1 d, while more than 40% of the biggest systems last more than 24 hours. Thus, there is a general positive relationship between the size of PLs, their duration and distance travelled. This finding translates, on average, to smaller PLs travelling shorter distances and having a reduced lifespan than larger systems.

3.2.2. PL speed of propagation and direction. Our WR approach also illuminates the relationship between PL tracks and the lower-atmosphere wind field (Fig. 12). The average speed of PL propagation of 8.75 m/s conceals the fact that some systems move as fast as 23 m/s, while for the vast majority (80%), propagation speeds range between 5 and 13 m/s (Fig. 9d). PLs can also change direction suddenly, as well as alternate between slow and fast periods, apparently in response to the lower level wind flow (see below).

In terms of the dominant direction of propagation, determined as a straight line connecting the formation and dissipation points of each system (Fig. 12), we note that the vast majority of PLs (70%) travel southward and the main direction is southeastward (41%). However, more than 25% of PLs travel westward and more than 20% propagate northward. There is very little change in these percentages across cold-season months. The displacement of PLs is substantially linked to WRs (Fig. 10d). PL tracks accompanying NAO+ average slower than other WR configurations, with more than 40% moving slower than 6 m/s (respectively 23%, 24%, 8% and 23% for AR, NAO−, SB and Others). Conversely, SB tracks are faster, with almost 70% of PLs moving at 9 m/s or more (respectively 45%, 35%, 26% and 47% for AR, NAO+, NAO− and Others) and with almost 25% reaching 15 m/s or more.

The main direction of PL tracks also differs according to WRs. There is a large difference between the negative phase of NAO and other WRs: during NAO− phases PL tracks are directed mainly southwestward (Fig. 12). Also, there are fewer PLs during SB periods; PLs during those periods tend to impact more the Norwegian coast, and travel almost exclusively eastwards. Overall, PLs travel in the dominant direction of the large-scale lower atmosphere (850 hPa) wind field, as shown for the AR pattern, for example (Fig. 13a). Equally the southwestward and eastward directions of PL tracks during NAO− and SB respectively show associations with the 850 hPa windflow (Fig. 13c and d).

3.3. Dual and multiple PL characteristics

In this section, we consider exclusively the vortices that were not included in the statistics and discussion of the previous section, to investigate whether dual and multiple PLs are different from the individual (deepest) lows. Of the 190 PL events in our study, 56 are dual, of which nine are classified as 'wave systems', and 24 are multiple, of which 8 events are classified as 'merry-go-round' (Forbes and Lottes, 1985). With the exception of the latter systems, dual and multiple systems exhibit roughly the same spatial and temporal distributions as other PLs in the list (Fig. 14a and b). All merry-go-round systems formed over the Norwegian Sea (between 71.5°N–74.5°N and 5.5°E–22.5°E) in January and March, except for one case that formed east of Iceland (68.E°N–13.5°W). Wave systems form preferentially over the Barents Sea (six over the Barents Sea between 71°N–75°N and 20°E–36°E, two over the Norwegian Sea and one near Iceland).

The atmospheric large-scale circulation (Table 2 and Fig. 14c) also seems to help determine the formation of multiple systems over Nordic Seas. Both the negative and positive phases of NAO appear more favourable for development
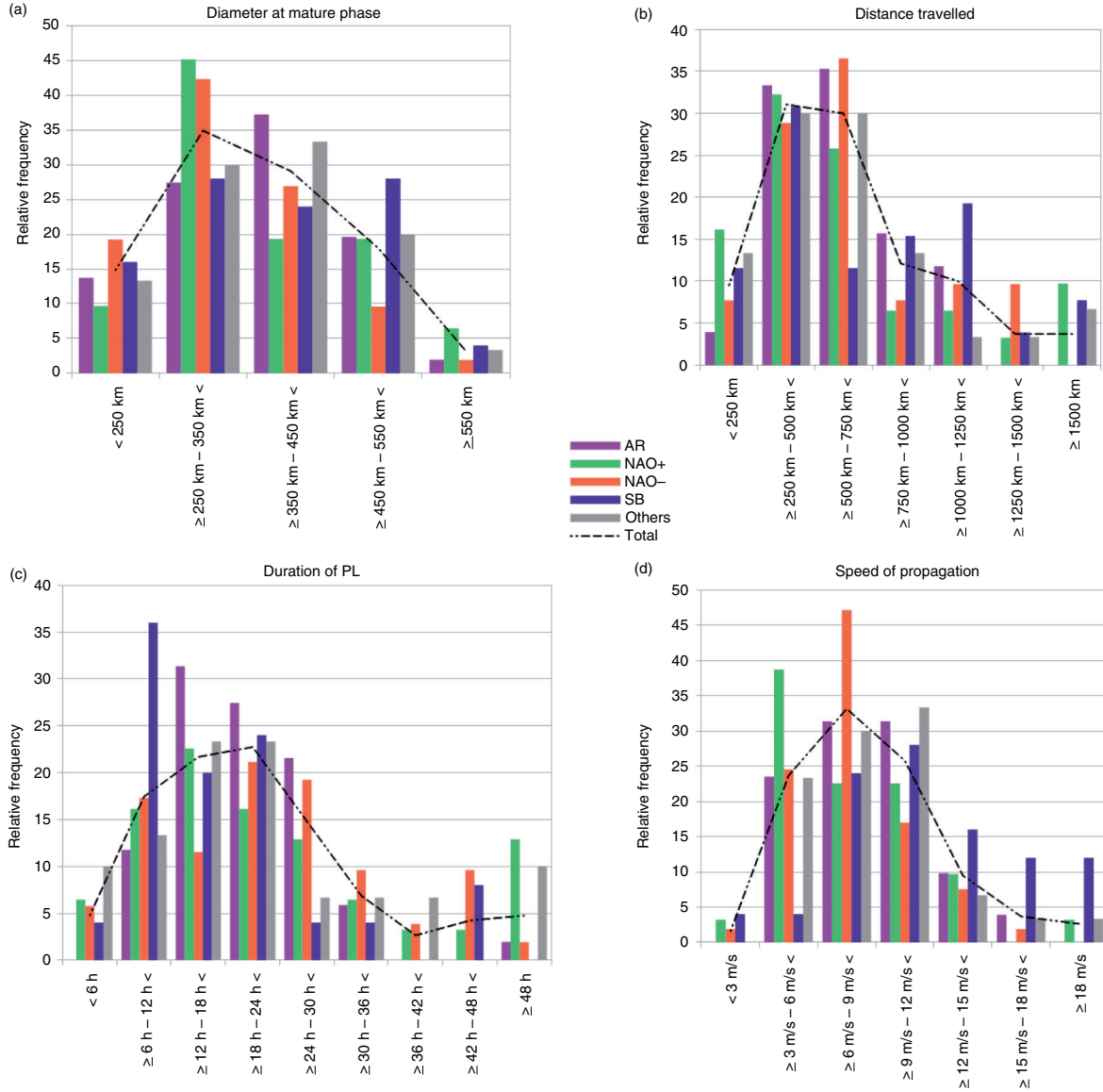
Fig. 10. PLs characteristics according to weather regimes. (a) diameters, (b) total distance travelled, (c) lifespan and (d) speed of propagation. Number of PLs per category: AR (51 PLs), NAO+ (31 PLs), NAO− (52 PLs), SB (26 PLs), Others (30) and Total (190 PLs).

of multiple PL events than the AR and SB WRs. This difference is particularly evident for the AR and NAO−; the most favourable regimes for PL formation in general (Mallet et al., 2013). Only 8% of multiple events occurred in the AR configuration while 40% of multiple systems occurred during NAO−.

As noted, PLs move in the direction of the large-scale flow of the lower troposphere. The same relationship is also observed for dual and multiple systems. In general, the larger-scale 850 hPa wind field compares favourably with the directions and speeds of dual and multiple systems. We note that for some, but not all, dual and multiple PL cases (not shown), their movement is also determined by the interactions between or among systems in their general vicinity (Renfrew et al., 1997).

To summarise, our analyses show preferential areas for the formation of dual and multiple PL systems (wave systems in the Barents Sea, merry-go-round systems in the Norwegian Sea). The occurrence of single systems is, to a considerable extent, related to the large-scale circulation (WRs), with PL spatial displacement highly influenced by the wind field of the lower troposphere. Multiple PLs
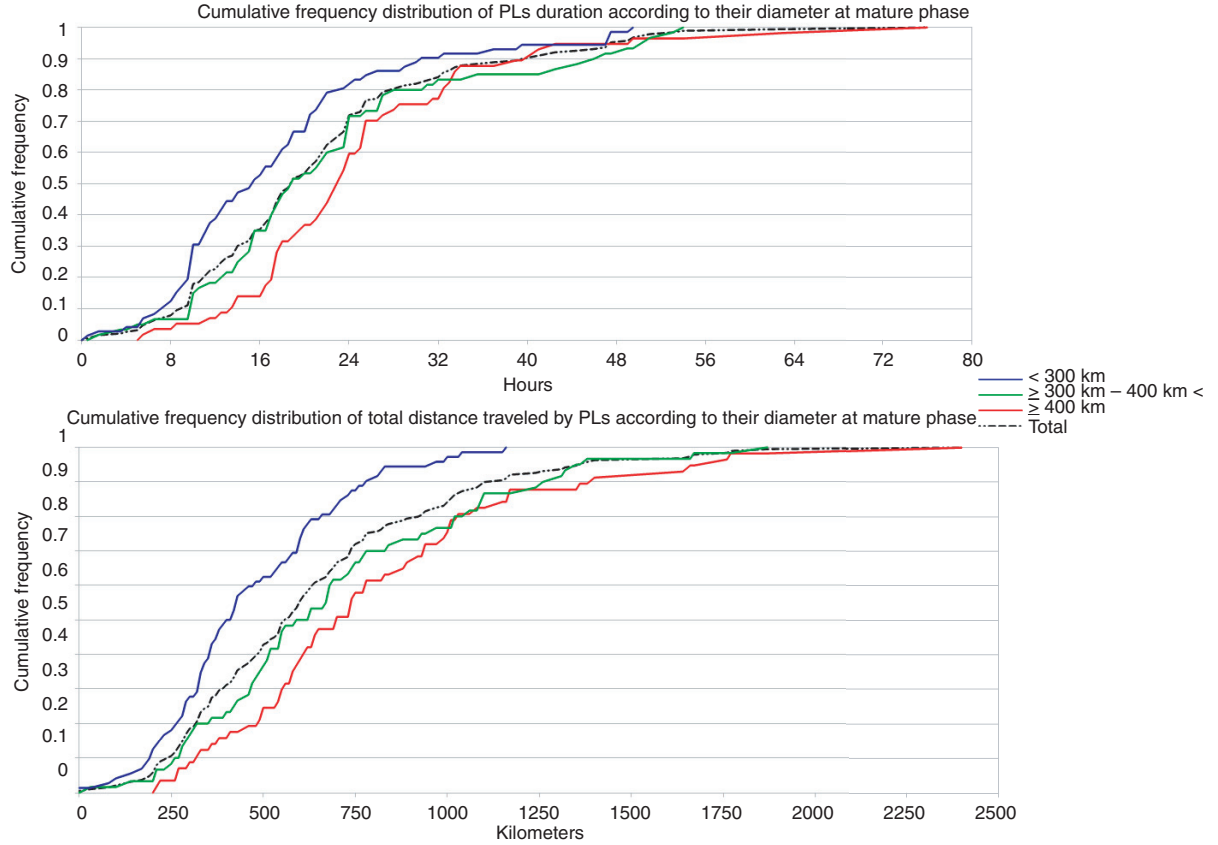
Fig. 11.   Cumulative frequency distribution of PL duration and total distance travelled according to size at the mature phase. Blue line represents PLs which do not exceed 300 km at mature phase, green line represents PLs between 300 and 400 km at mature phase, red line represents PLs which exceed 400 km at mature phase and the black dashed line represents all the PLs observed in our study.

exhibit similar behaviour to the deepest individual low; thus, to exclude them from the statistics on single PLs is not a limitation of our study.

4. Discussion

Our investigation of the tracks and lifespan characteristics of PLs over Nordic Seas for the 14-yr period 1999–2000 to 2012–2013, relies upon manual tracking of their cloud signatures appearing on satellite images, from their points of genesis until dissipation. In the large study region comprising our analysis, we identify a strong tendency for PLs to form coincident with the (NAC, WSC and Barents Sea currents), and to move following the larger-scale lower-atmospheric wind field. This is an expected finding, consistent with dynamical and thermodynamic considerations. The strong inter-annual variability of PLs that we note, along with more activity in the second half of the study period for late winter (February, March and April), also shows up in comparisons with the shorter period 2000–2009 of Noer et al. (2011).

A change in the seasonal evolution of sea-ice extent may at least partly explain the recent increase of PLs that we note for the Greenland Sea – west of Spitsbergen – and over the Barents Sea. The decreased sea-ice extent of the Barents Sea (Comiso, 2011; Årthun et al., 2012) likely offers favourable atmospheric and upper oceanic conditions for the increased PL development there in the second period. Our finding of, on average, approximately 14 PLs forming per winter – ranging from a maximum of 23 in 2012–2013 to a minimum of 5 in 1999–2000 – differs notably from Blechschmidt (2008), who observed about 90 PLs over a 2-yr period. However, this difference can likely be attributed to the fact that Blechschmidt considered a much larger area (extending to the west to Cape Farewell), analysed for the whole year, and with a less conservative definition of PLs compared to the criteria used in the present study (see Subsection 2.1). Possibly, the inclusion of mesocyclones of bigger horizontal scales (until 1000 km) or that are not associated with a CAO might have helped lead to more PLs being counted in the Blechschmidt study.

Previous PL studies for the Nordic Seas indicate clearly a February minimum in PL frequency (Wilhelmsen, 1985,
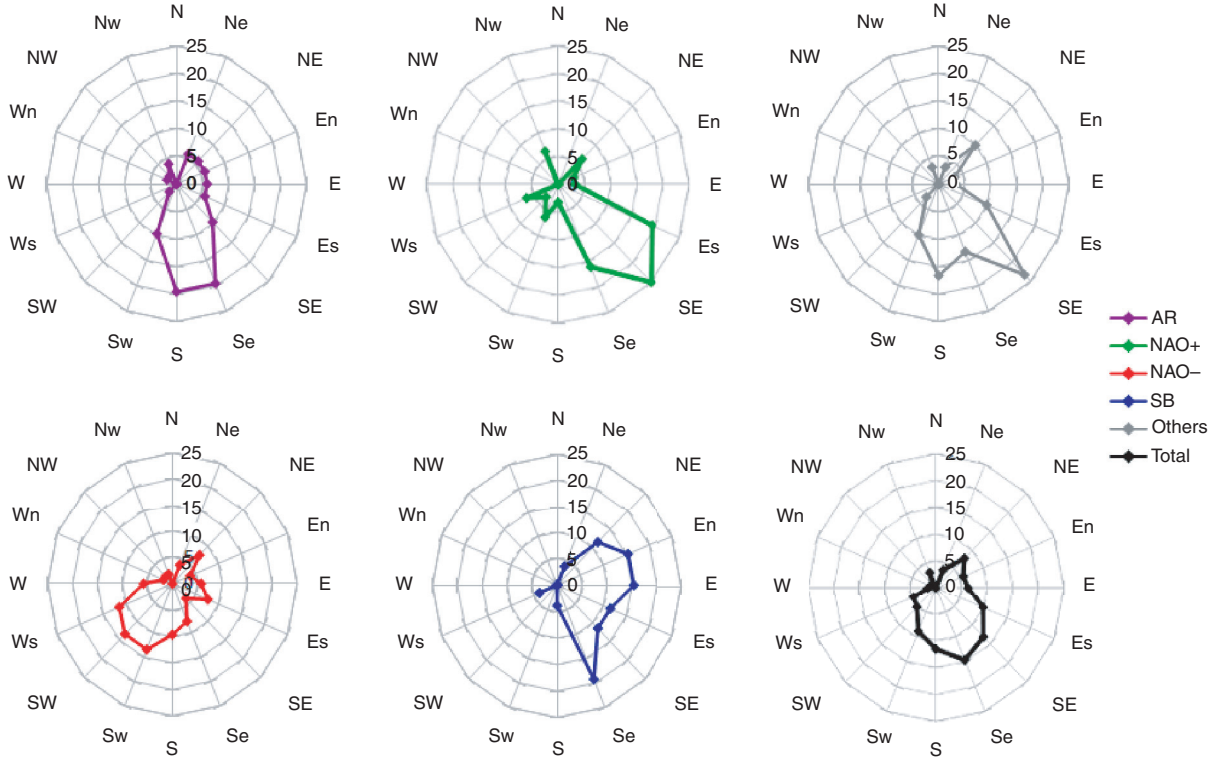
Fig. 12. Main directions (in percentage) of PLs over the Nordic Seas from winter 1999/2000 to winter 2012/2013, stratified by weather regimes.

Noer et al., 2011), which is also seen when considering the 14-winter period but not as pronounced. More specifically, Wilhelmsen (1985) found two winter sub-periods with high PL frequency, the first between November and January with a maximum in December, and then between March and April. However, in Noer et al. (2011), the main period of PL development was from November to March with a maximum in January. Note that Noer et al. (2011) investigated the same area as ours only for a shorter period (2000–2009), while Wilhelmsen (1985) studied PLs of the Norwegian Sea and Barents Sea making landfall between 1972 and 1982. We note that, for the second sub-period of our study (September 2006 to May 2013), the frequency of PLs is high from January to April, without a local minimum in February and a marked maximum in March (Fig. 4b). In the most recent years of the updated Noer and Lien (2010) there may have been a change in when the maximum PL frequency occurs but only a forward extension of the dataset can clarify this possibility.

Although we confirm that most PLs move southward or southeastward, steered by the synoptic-scale lower- tropospheric flow, we note that a substantial number have a westward or even northward trajectory (20% of PLs exhibit a westward trajectory and 20% exhibit a northward trajectory). Therefore, in studies that automatically detect

PLs, an imposed southward movement in models (Zahn and von Storch, 2008) may miss some systems.

The evidence we present for an association between WRs and PL movement, in terms of their dominant direction and speed of propagation, might potentially help improve prediction of PL occurrences and tracks on short to medium time scales. For instance, the PLs accompanying the SB configuration are moving mainly eastward, and average faster speeds probably because of the strong westerly near-surface wind flow (850 hPa) over Nordic Seas (Fig. 13d). Conversely, the large-scale wind flow at 850 hPa during NAO+ configuration, displayed on Fig. 13b, is shown to be weak over the Norwegian and Barents Seas, and may explain why PLs accompanying this WR average slower than other PLs. Moreover, PLs occurring over the Barents Sea during the AR, NAO − and NAO+ configurations move slower than other PLs in adjacent regions during these same WRs, which is likely linked to the weaker near surface winds over the Barents Sea during these WRs (Fig. 13a, b and c.)

The PLs accompanying the AR configuration mostly form at the convergence of the NAC and the WSC over the northeastern Norwegian Sea (Fig. 8a), possibly making landfall more often than during other WRs because of the north and north-westerly low troposphere (850 hPa) wind flow over this area (Fig. 13a). Conversely, the north-easterly wind flow
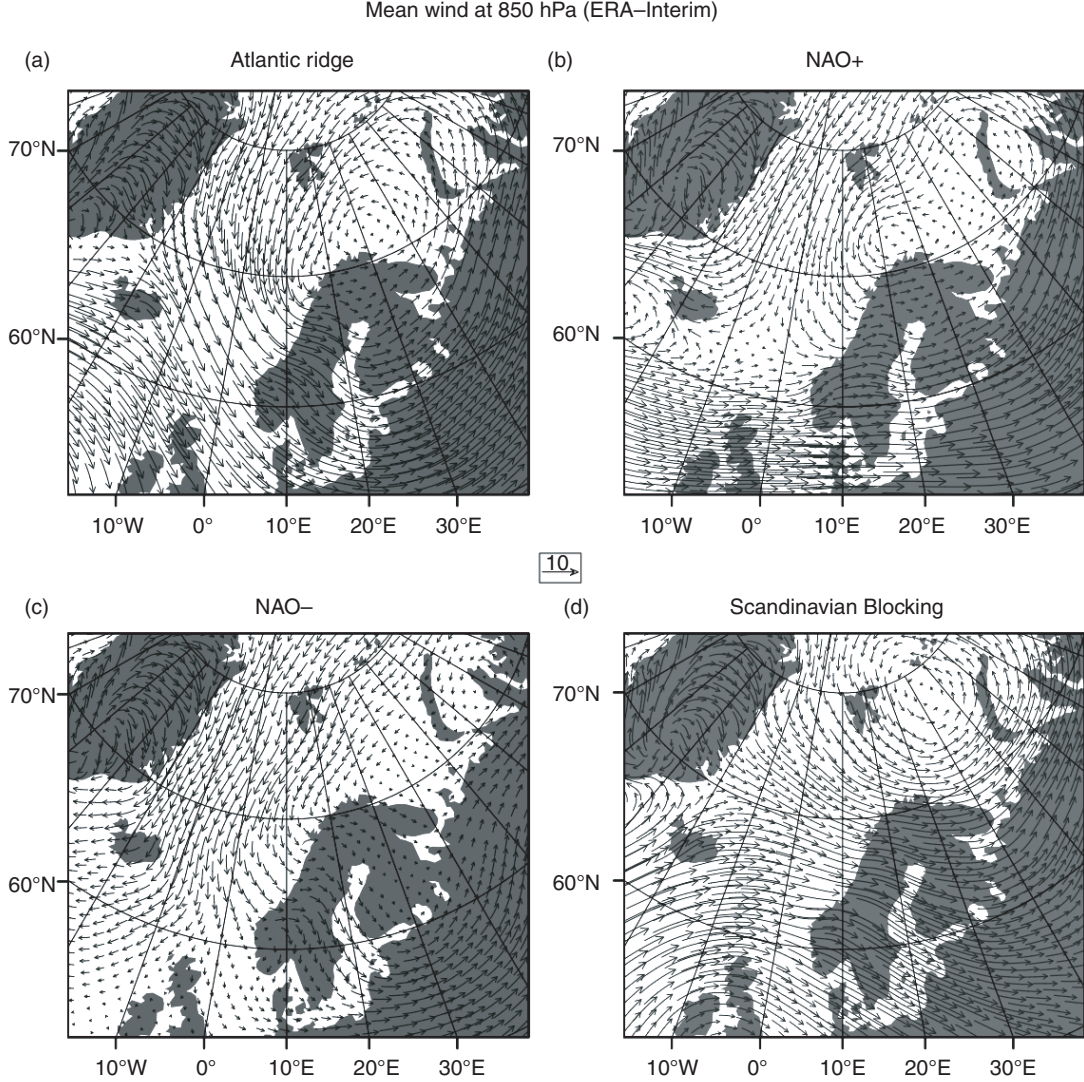
Mean wind at 850 hPa (ERA–Interim)

Fig. 13.   Composite mean wind field at 850 hPa for PL events accompanying (a) AR, (b) NAO+, (c) NAO − and (d) SB configurations.

at 850 hPa during the negative phase of the NAO (Fig. 13c) likely limits the risk of PL landfalls (Fig. 8c). This information can potentially help improve predictability of PLs and, therefore, their hazards to the Nordic Seas and surrounding areas, on short to medium time scales.

Our finding that PLs forming over Barents Sea travel shorter distances may possibly be the result of a narrow open-sea area, especially at the end of the winter when sea-ice reaches its maximum extent and most PLs occur in this area.

Finally, the exclusion of auxiliary systems in the case of multiple vortices from our analysis is justified by the fact that the wind within the system may not reach a speed sufficient to be classified as PLs. However, this is not considered a limitation of our study because of our finding that dual and multiple systems exhibit broadly similar

spatio-temporal characteristics than the deepest individual PLs. To the knowledge of the authors, this is the first study that specifically investigates these auxiliary systems over a 14 winter period. Here again, a forward extension of the dataset is highly desirable to confirm the results obtained in this study.

5. Conclusion

PLs are an important phenomenon of the higher-latitude weather and climate systems that are frequently difficult to forecast, given their relatively small size, rapid development, and formation over the ocean away from a high density of conventional observing sites.

We undertook a 14-winter climatic analysis of PL tracks and other attributes (e.g. duration, lifespan) for the Nordic
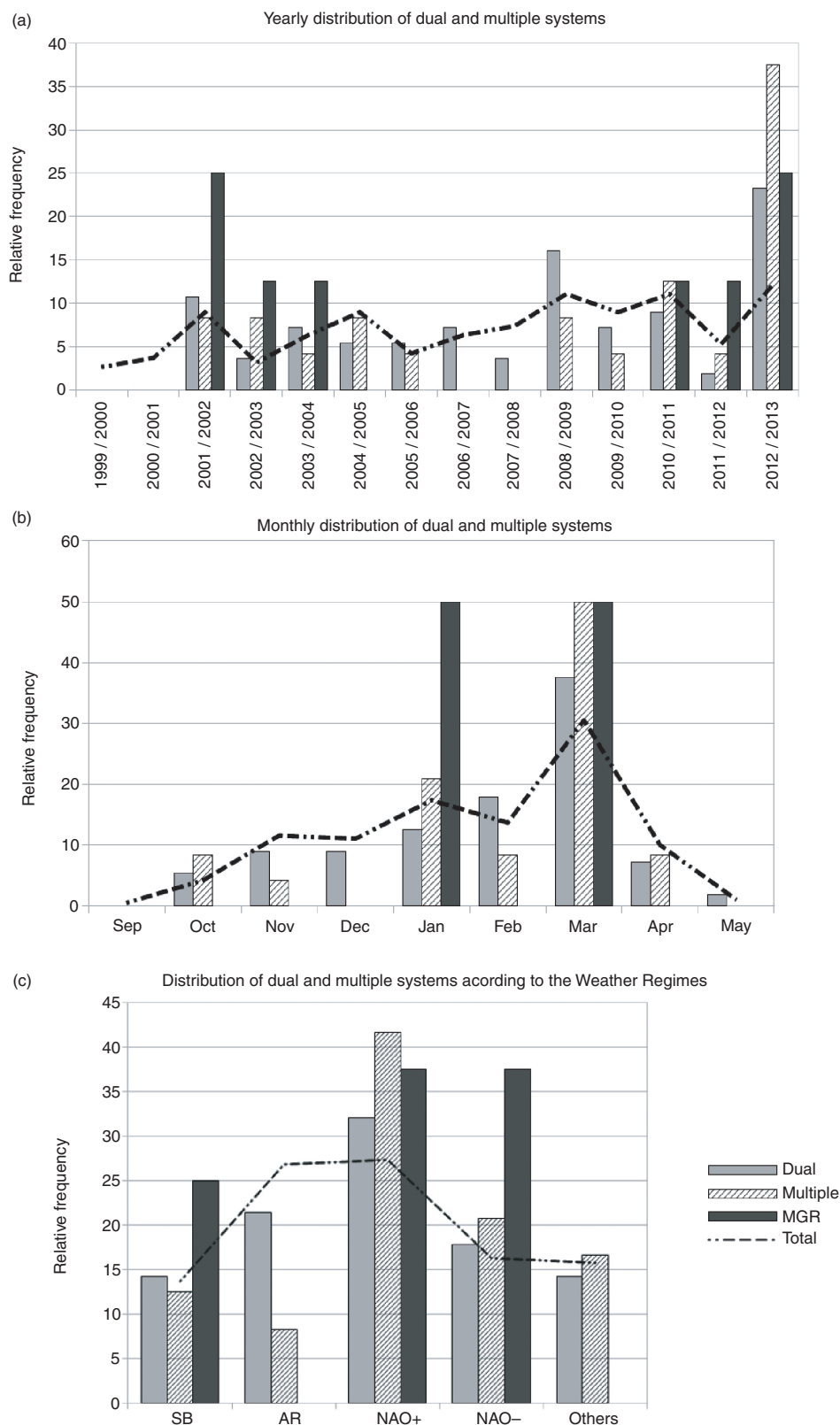
(a)

(b)

(c)

Fig. 14. Distribution (in percentage) of dual and multiple systems over Nordic Seas during the period 1999/2000 to 2012/2013. Parts (a) and (b) display the temporal distribution; (c) shows the distribution according to WRs.

Table 2. Frequency of dual and multiple PLs over the Nordic Seas according to weather regimes

	AR	NAO +	NAO −	SB	Others	Total
Dual	8	10	18	12	8	56
Multiple	2	5	10	3	4	24
Dual relative frequency	14	18	32	21	14	100
Multiple relative frequency	8	21	42	13	17	100

Seas, using a detailed inventory of systems derived from the analysis of surface observations and satellite TIR images. The study results confirm previous shorter-duration or smaller-region studies, as follows:

- PLs develop and travel over all open water areas of the Nordic Seas;
- PL density is greatest at the convergence of the NAC and the WSC, and the NAC and Barents Sea currents. About 25% of PLs form in areas relatively close to the ice edge;
- The mean diameter of mature PLs is 350 km, with two-thirds of systems in the range 250 km to just under 450 km.
- Most systems last less than 24 hours but on occasion can endure for more than 48 hours.
- The distance travelled by PLs can reach 2000 km, although more than 80% travelled less than 1000 km during their lifespan.

The present study results also increase our knowledge of PLs in this region, particularly as follows:

- The PL genesis area shifts from the western to the eastern North Atlantic between the beginning and the end of the cold season;
- For the most recent period, the local frequency minimum in February is absent and the maximum is reached in March, possibly indicating multi-annual or even decadal variability;
- PLs in the western part of the region average larger than their eastern counterparts. There is a positive relationship between the size of PLs, their duration and distance travelled, such that larger systems also tend to last longer and travel further. Conversely, in the Barents Sea, systems are generally smaller and travel shorter distances;
- A substantial number (20%) of PLs in the Nordic Seas track northward;
- PL characteristics (size and lifespan) and tracks (direction and propagation speed) differ according to WRs. PLs forming during the negative phase of NAO average smaller diameters than for other configurations. Although PLs move mainly southward and southeastward, they mostly move eastward during SB configuration and southwestward during NAO −. PLs accompanying the SB configuration also average a faster rate of travel than for other WRs;
- Dual and multiple PLs have generally similar spatio-temporal characteristics to single PLs. Wave systems are more commonly found over the Barents Sea, while merry-go-round systems occur over the Norwegian Sea.

A forward extension of the Noer and Lien (2010) list, and its subsequent analysis in the future, will permit both the derivation of a PL climatology for the Nordic Seas region, and a fuller assessment of PL inter-annual and multi-annual variations.

6. Acknowledgements

References

Årthun, M., Eldevik, T., Smedsrud, L. H., Skagseth, Ø. and Ingvaldsen, R. B. 2012. Quantifying the influence of Atlantic heat on Barents Sea ice variability and retreat. *J. Clim.* **25**, 4736–4743.

Blechschmidt, A.-M. 2008. A 2-year climatology of polar low events over the Nordic Seas from satellite remote sensing. *Geophys. Res. Lett.* **35**(9), L09815. DOI: 10.1029/2008GL033706.

Blechschmidt, A.-M., Bakan, S. and Graßl, H. 2009. Large-scale atmospheric circulation patterns during polar low events over the Nordic seas. *J. Geophys. Res.* **114**, D06115. DOI: 10.1029/2008JD010865.

Businger, S. 1985. The synoptic climatology of polar low outbreaks. *Tellus A.* **37**, 419–432.

Bracegirdle, T. J. and Gray, S. L. 2008. An objective climatology of the dynamical forcing of polar lows in the Nordic seas. *Int. J. Clim.* **28**, 1903–1919.

Carleton, A. M. 1985. Satellite climatological aspects of the "polar low" and "instant occlusion". *Tellus A.* **37**, 433–450.

Carleton, A. M. 1987. Satellite-derived attributes of cloud vortex systems and their application to climate studies. *Remote Sens. Environ.* **22**, 271–296.

Carleton, A. M. 1995. On the interpretation and classification of mesoscale cyclones from satellite IR imagery. *Int. J. Remote Sens.* **16**, 2457–2485.

Carleton, A. M. 1996. Satellite climatological aspects of cold air mesocyclones in the Arctic and Antarctic. *Global Atmos Ocean Syst.* **5**, 1–42.

Cassou, C. 2008. Intraseasonal interaction between the Madden-Julian Oscillation and the North Atlantic Oscillation. *Nature.* **455**, 523–527. DOI: 10.1038/nature07286.

Claud, C., Duchiron, B. and Terray, P. 2007. Associations between large-scale atmospheric circulation and polar low developments over the North Atlantic during winter. *J. Geophys. Res.* **112**, D12101.

Claud, C., Heinemann, G., Raustein, E. and McMurdie, L. 2004. Polar low le Cygne: satellite observations and numerical simulations. *Q. J. Roy. Meteorol. Soc.* **130**, 1075–1102. DOI: 10.1256/qj.03.72.

Claud, C., Katsaros, K. B., Petty, G. W., Chedin, A. and Scott, N. A. 1992. A cold air outbreak over the Norwegian Sea observed with the TIROS-N Operational Vertical Sounder (TOVS) and the Special Sensor Microwave Imager (SSM/I). *Tellus A.* **44**, 100–118.

Comiso, J. C. 2011. Large decadal decline of the Arctic multiyear ice cover. *J. Clim.* **25**, 1176–1193. DOI: 10.1175/JCLI-D-11-00113.1.

Dee, D. P., Uppala, S. M., Simmons, A. J., Berrisford, P., Poli, P. and co-authors. 2011. The ERA-Interim reanalysis: configuration and performance of the data assimilation system. *Q. J. Roy. Meteorol. Soc.* **137**, 553–597.

Dysthe, K. B. and Harbitz, A. 1987. Big waves from polar lows? *Tellus A.* **37**, 500–508.

Eidsvik, K. J. 1987. Predicted hazard area for a polar low. *Tellus A.* **39A**, 390–396.

Ese, T., Kanestrom, I. and Pedersen, K. 1988. Climatology of polar lows over the Norwegian and Barents Sea. *Tellus A.* **40**, 248–255.

Fitch, M. and Carleton, A. M. 1991. Antarctic mesocyclone regimes from satellite and conventional data. *Tellus A.* **44**, 180–196.

Forbes, G. S. and Lottes, W. D. 1985. Classification of mesoscale vortices in polar airstreams and the influence of the large-scale environment on their evolutions. *Tellus A.* **37**, 132–155.

Harold, J., Bigg, G. and Turner, J. 1999. Mesocyclone activity over the north-east Atlantic. Part 1: Vortex distribution and variability. *Int. J. Clim.* **19**, 1187–1204.

Heinemann, G. and Claud, C. 1997. Report of a workshop on "Theoretical and observational studies of polar lows" of the European Geophysical Society Polar Lows Working Group. *Bull. Am. Meteorol. Soc.* **78**, 2643–2658.

Kalnay, E., Kanamitsu, M., Kistler, R., Collins, W., Deaven, D. and co-authors. 1996. The NCEP/NCAR 40-year reanalysis project. *Bull. Am. Meteorol. Soc.* **77**(3), 437–471.

Laffineur, T., Claud, C., Chaboureau, J.-P. and Noer, G. 2014. Polar lows over the Nordic Seas: improved representation in ERA-Interim compared to ERA-40 and the impact on downscaled simulations. *Mon. Weather Rev.* **142**, 2271–2289. DOI: 10.1175/MWR-D-13-00171.1.

Mallet, P.-E., Claud, C., Cassou, C., Noer, G. and Kodera, K. 2013. Polar lows over the Nordic and Labrador Seas: synoptic circulation patterns and associations with North Atlantic-Europe wintertime weather regimes. *J. Geophys. Res. Atmos.* **118**(6), 2455–2472.

Noer, G. and Lien, T. 2010. Dates and positions of Polar Lows over the Nordic Seas between 2000 and 2010. Met.no report 16/2010.

Noer, G., Saetra, O., Lien, T. and Gusdal, Y. 2011. A climatological study of polar lows in the Nordic Seas. *Q. J. Roy. Meteorol. Soc.* **137**, 1762–1772.

Rasmussen, E. A. and Turner, J. 2003. Introduction. In: *Polar Lows: Mesoscale Weather Systems in the Polar Regions* (eds. E. A. Rasmussen and J. Turner), Cambridge University Press, Cambridge, pp. 1–51.

Renfrew, I. A., Moore, G. W. K. and Clerk, A. A. 1997. Binary interactions between polar lows. *Tellus A.* **47**, 577–594.

Wilhelmsen, K. 1985. Climatological study of gale-producing polar low near Norway. *Tellus A.* **37**, 451–459.

Zahn, M. and von Storch, H. 2008. A long-term climatology of North Atlantic polar lows. *Geophys. Res. Lett.* **35**(22), L22702. DOI: 10.1029/2008GL035769.

Zappa, G., Shaffrey, L. and Hodges, K. 2014. Can polar lows be objectively identified and tracked in the ECMWF operational analysis and the ERA-Interim reanalysis? *Mon. Weather Rev.* **142**(8), 2596–2608. DOI: 10.1175/MWR-D-14-00064.1.